ELSEVIER
SAUNDERS

Radiol Clin N Am 43 (2005) 169 – 187

RADIOLOGIC
CLINICS
of North America

Imaging hypoxia and angiogenesis in tumors

Joseph G. Rajendran, MD[a,b,*], Kenneth A. Krohn, PhD[a,b]

[a]*Division of Nuclear Medicine, Department of Radiology, Box 356113, University of Washington, Seattle, WA 98195, USA*
[b]*Department of Radiation Oncology, University of Washington, Seattle, WA, USA*

Advances in molecular imaging are rapidly changing the paradigm for noninvasive diagnostic imaging from largely morphologic methods to ones that include both anatomy and parameters of function, overcoming some of the limitations of previous imaging modalities [1–5]. This paradigm allows clinicians to provide more comprehensive patient evaluation serially and in a noninvasive fashion. Advances in PET imaging instrumentation, coupled with the development of an increasing pharmacopoeia of molecular probes, have been driving forces for the rapid changes that are taking place in molecular medicine [6–9]. These advances are necessary to keep pace with the increasing sophistication of clinical questions asked of imaging specialists.

The physiologic environment for a tumor is different from normal tissue. It exhibits an evolving microenvironment that is largely dictated by abnormal vasculature and metabolism that is disease specific. One of these changes in tissue microenvironment is hypoxia, a state of reduced oxygenation in tissues. Oxygen is an essential metabolic substrate because of its critical role as the terminal electron acceptor in metabolic respiration. Levels of oxygen range through a continuum between normal levels (euoxia or normoxia) and total lack of oxygen (anoxia). The tissue oxygen levels, commonly reported as Po_2 can reach as low as less than 5 mm Hg and cells can still survive and adapt to these circumstances.

Ischemia and hypoxia are not synonymous; the former is a lack of perfusion and can lead to hypoxia, although it may not be evident until the late stages of ischemia. Tissue hypoxia can also be present in the absence of significant ischemia. Many solid tumors develop areas of hypoxia during their evolution. This is primarily caused by unregulated cellular growth, resulting in a greater demand on oxygen for energy metabolism. High interstitial pressure may exacerbate the already inefficient vascularization within the tumor [10]. In addition, other factors, such as low O_2 solubility (anemia), might increase levels of tissue hypoxia. Clinicians owe an understanding of the mechanistic aspects of hypoxia as a variable in response to cancer therapy to Thomlinson and Gray [11], who in the last century showed the impact of a distance greater than 200 μm from a capillary on cell viability and survival (Fig. 1).

Hypoxia-induced changes in tumor biology

Aggressive tumors often have high microvessel density but even higher levels of hypoxia [12]. The attempt by hypoxic cells to use glycolysis to maintain adequate cellular levels of ATP in the absence of oxygen is, however, ineffective compared with oxidative phosphorylation under normoxic conditions. As a consequence of increased glycolysis, cells accumulate lactate, with a consequent change in pH and decreased ATP:ADP ratio. Calcium homeostasis is also impaired. Ca^{++} leaves the mitochondria for the cytosolic space, and ATPase is perturbed with K^+ loss and Na^+ loading. Poor delivery of oxygen to the

This study was supported in part by National Institutes of Health Grant P01 CA42045.

* Corresponding author. Division of Nuclear Medicine, Department of Radiology, Box 356113, University of Washington, Seattle, WA 98195.

E-mail address: rajan@u.washington.edu (J.G. Rajendran).

0033-8389/05/$ – see front matter
doi:10.1016/j.rcl.2004.08.004

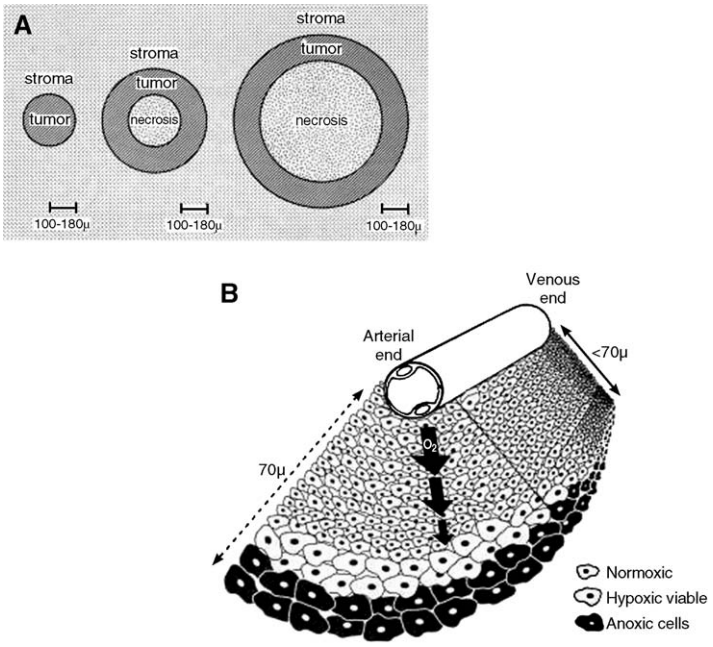

Fig. 1. (*A*) Diagrammatic illustration of the conclusions of Thomlinson and Gray from their study of human bronchogenic carcinoma. The degree of necrosis is a function of the distance from the capillaries. (*B*) Diffusion of oxygen from a capillary through tumor tissue resulting in a gradient of oxygenation and the presence of a sequential range of normoxic to anoxic cells through intermediate hypoxic but viable cells. (*From* Hall EJ. Radiobiology for the radiologist. Philadelphia: Lippincott Williams & Wilkins; 2000. p. 141; with permission.)

tumor eventually leads to a lack of glycolytic activity, even in the presence of hypoxia, a fact that can have profound implications for using fluorodeoxyglucose (FDG) as a surrogate marker for hypoxia (Fig. 2) [13].

Irrespective of the level of perfusion or status of the vasculature in a tumor, hypoxia induces changes that reflect homeostatic attempts to maintain adequate oxygenation by increasing extraction from blood and by inducing cells to adapt by developing more

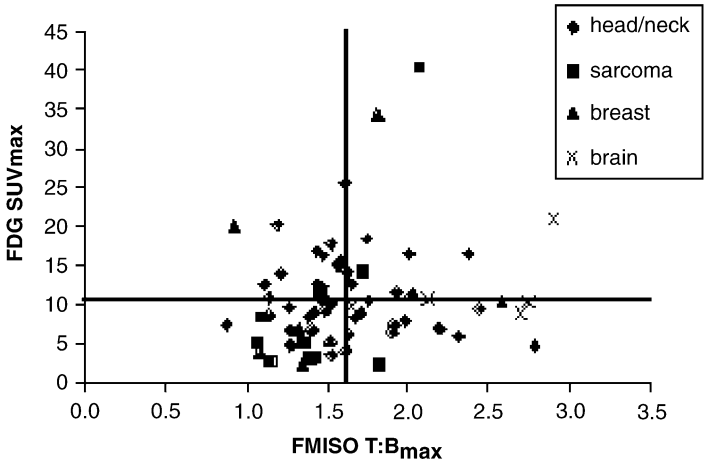

Fig. 2. Graph showing the distribution of FDG and [^{18}F]-fluoromisonidazole (FMISO) uptake (divided into four quadrants based on the median uptake values) in patients with several types of cancer. This shows the heterogeneous correlation between hypoxia and glycolysis.

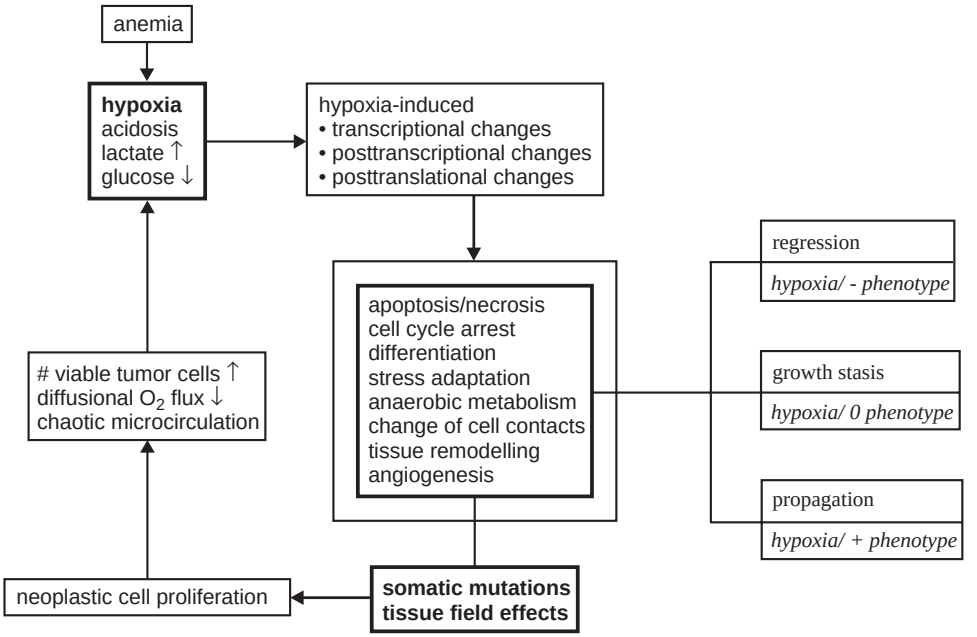

Fig. 3. Hypoxia-induced proteomic changes in cancer cells influencing propagation of cancer. The net result of these effects is manifested by growth, regression, or stable disease. (*From* Hockel M, Vaupel P. Tumor hypoxia: definitions and current clinical, biologic, and molecular aspects. J Natl Cancer Inst 2001;93:266; with permission.)

aggressive survival traits through expression of new proteins. A number of hypoxia-related genes are responsible for these genomic changes and are mediated by downstream transcription factors that have been identified (Figs. 3 and 4) [14–17]. These include expression of endothelial cytokines, such as vascular endothelial growth factor, and signaling molecules, such as interleukin-1, tumor necrosis factor-α, and transforming growth factor-β,and selection of cells with mutant p53 expression [18,19]. Several consequences of this genetic adaptation are relevant to treatment and imaging. For example,

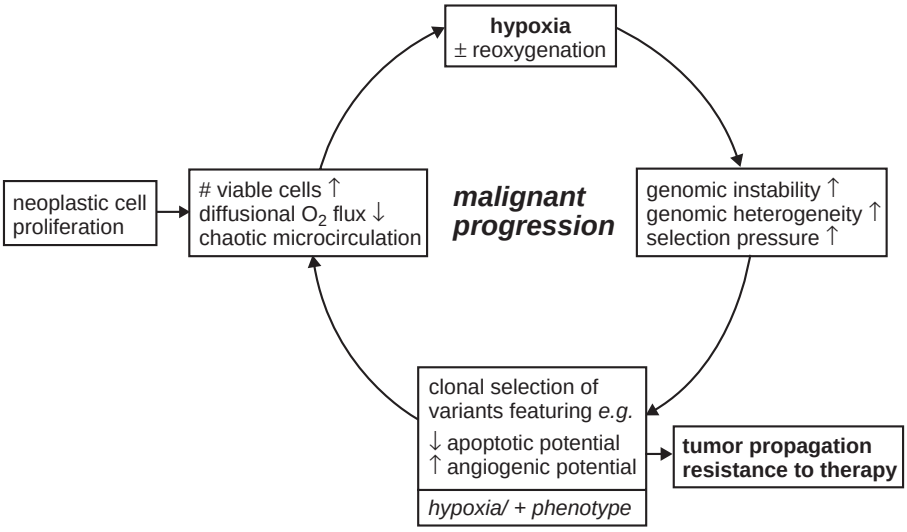

Fig. 4. Progressive genomic changes in a tumor resulting from hypoxia. (*From* Hockel M, Vaupel P. Tumor hypoxia: definitions and current clinical, biologic, and molecular aspects. J Natl Cancer Inst 2001;93:266–76; with permission.)

hypoxic cells do not readily undergo death by apoptosis [20] or arrest in G1 phase of the cell cycle in response to sublethal DNA damage [21,22]. Increased glucose transporter activity is responsible for much of the increased glucose uptake associated with hypoxia, which can be as high as twofold [23,24].

Hypoxia-inducible factor

Mechanistic aspects of tissue oxygen sensing and hypoxia response are areas of active investigation. The primary cellular oxygen-sensing mechanism seems to be mediated by a heme protein that uses O_2 as a substrate to catalyze hydroxylation of proline in a segment of hypoxia-inducible factor (HIF)-1α. This leads to rapid degradation of HIF-1α under normoxic conditions. [25]. In the absence of O_2, HIF-1α accumulates and forms a heterodimer with HIF-1β that is transported to the nucleus and promotes hypoxia-responsive genes, resulting in a cascade of genetic and metabolic events in an effort to mitigate the effects of hypoxia on cellular energetics [21,26]. Stabilization of HIF-1α has been shown to occur early in the process of tumor development [27]. Measurement of overexpressed HIF-1α in tissues by immunocytochemical staining can be used as an indirect measure of hypoxia [28–30] but its heterogeneous expression within a tumor limits the value of immunocytochemical staining.

Angiogenesis

Angiogenesis, the formation of new blood vessels, is an important aspect of the tumor phenotype. It is essential to deliver nutrients for tumor growth, invasion, and metastatic spread. It is an independent prognostic marker and, because vascular endothelial cells are more genetically stable than tumor cells, it is an attractive target for new treatment strategies. In simple terms, angiogenesis is a failure of the balance between proangiogenic and antiangiogenic signals. Angiogenesis that is commonly seen in neoplasia is another consequence of microenvironmental factors. Tumors switch to angiogenesis under a variety of stress signals, which results in tumor growth and metastases. As a general rule, tumors do not grow beyond a size of 1 to 2 mm without producing new blood vessels [31]. The network of blood vessels formed in a tumor can show significant functional deficiencies compared with normal vasculature [10,32] and these distinctions can be exploited for imaging. The angiogenesis trigger in tumor leads to new vessels with capillary endothelial cells with characteristics not found in normal tissues [33].

The emergence of angiogenesis as an important target for cancer therapy has prompted a great deal of new research to understand this molecular process. Gene expression profiling has identified proteins that are selectively expressed by tumor endothelial cells, including a large class of integrins, such as $\alpha_V\beta_3$ and $\alpha_V\beta_5$. These provide the potential for specific targeting of therapeutics [34]. This has coincided with the development of molecular imaging methods that provide the potential to monitor treatment [35,36]. Although angiogenesis is a frequent consequence of hypoxia, some tumors develop extensive angiogenesis without the presence of hypoxia and vice versa. A cause and effect relationship does not always exist. Kourkourakis et al [37] found a U-shaped association between the two phenomena, which was explained mechanistically. Prognosis has been found to be poor when there is poor angiogenesis, perhaps because of the presence of hypoxia or when there is profound angiogenesis, likely because of increased metastatic potential.

One example of de novo angiogenesis is seen in von Hippel-Lindau disease. Spontaneous renal tumors develop with overexpression of HIF-1α, resulting in widespread angiogenesis in the absence of hypoxia. Despite aggressive angiogenesis in many tumors and contrary to expectations, observed blood perfusion rates are lower in the tumor bed than in normal tissue. Moreover, as tumors grow, perfusion is further decreased because of a number of other biophysical parameters [35,38]. Immunocytochemical staining has also been used in evaluating angiogenesis in a tumor that results from some of the previously mentioned molecular changes, specifically the expression of vascular endothelial growth factor [19]. Neither perfusion nor permeability are adequate measure of angiogenesis.

Tumor hypoxia and clinical outcome: what is new?

Radiobiologists have long taught that low levels of intracellular oxygen result in poor response to radiation therapy. Oxygen is important for fixing, in the sense of making permanent, the radiation-induced cytotoxic products in tissues. In its absence, the free radicals formed by ionizing radiation recombine without producing the anticipated cellular damage

[39–41]. As a result, radiation oncologists have been frustrated by the fact that hypoxic tumors are not effectively eradicated with conventional doses of radiation. Clinical and preclinical experience indicates that it can take three times as much photon radiation dose to cause the same cytotoxic effect in hypoxic cells as compared with normoxic cells (Fig. 5) [41–44].

Although all these are established concepts, what is new is that hypoxia results in the development and selection of an aggressive phenotype, resulting in poor response and poor outcome because of increased metastatic potential [20,45–47]. Hypoxia has also been found to promote resistance to a number of chemotherapeutic agents by one or more independent mechanisms: (1) hypoxia can induce slowing of cellular proliferation, (2) changes in perfusion associated with hypoxia may impede delivery of chemotherapy drugs, and (3) gene amplification results in the induction of numerous stress proteins that are factors in limiting response [47,48].

Cancer treatment schemes designed to circumvent the cure-limiting consequences of hypoxia have led, however, to disappointing results [49]. Hyperbaric oxygen, neutron therapy, hyperfractionation, and the use of oxygen-mimetic radiation sensitizers have not had the anticipated clinical benefit. As promising as they may sound, these methods were associated with problems of either lack of widespread availability or serious clinical toxicity or they are simply ineffective in human trials. Authors have suggested several reasons for this lack of benefit. Especially relevant to this article is the probability that an assay is needed to select patients with hypoxia. A benefit in an appropriately selected patient population would be expected and the hypoxia assay could also be used to follow the response to treatment.

Hypoxic cells are attractive targets for hypoxia-activated prodrugs [50,51]. Newer hypoxia-activated prodrugs [52] are less toxic and more effective than their early counterparts, such as mitomycin C [53]. In addition to producing direct cytotoxic effects, these agents exhibit synergistic toxicity when used with radiation and chemotherapy. Although focal hypoxia in a tumor can be treated with boost radiation using intensity-modulated radiotherapy [54,55], more diffuse hypoxia benefits from hypoxic cell toxins and sensitizers. Nuclear imaging with hypoxia-specific tracers should be an important tool for selecting patients who might benefit from this treatment [56].

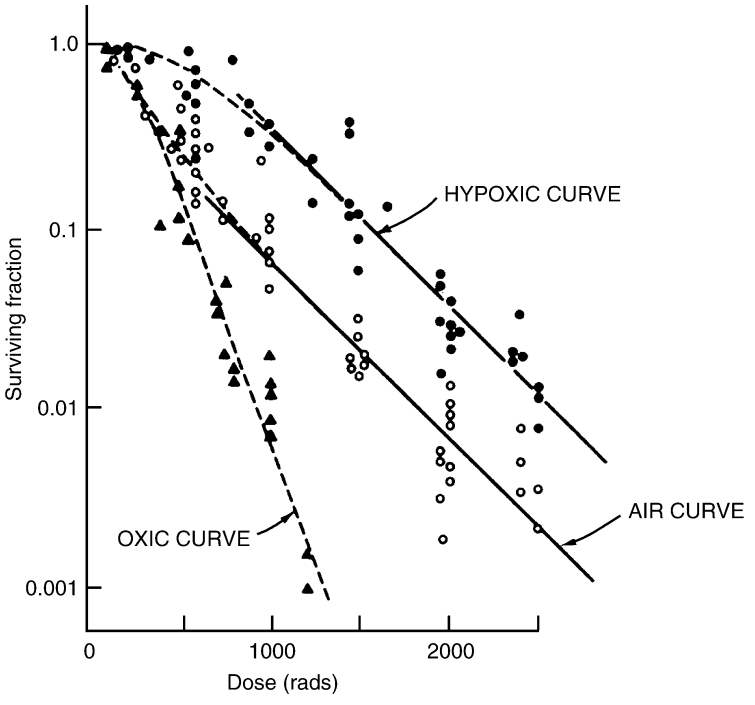

Fig. 5. This illustrates the relative resistance of hypoxic cells to radiation. In comparison with oxygenated cells hypoxic cells require three times more radiation to have the same effect. (*From* Hall EJ. Radiobiology for the radiologist. Philadelphia: Lippincott Williams & Wilkins; 2000. p. 145; with permission.)

The importance of selecting appropriate patients for a hypoxia-directed therapy results in the greatest benefit for the individual patient.

Need to identify hypoxia in tumors

The negative association of hypoxia with response to treatment and clinical outcome strongly implies that evaluating hypoxia helps in identifying tumors with a high hypoxic fraction so that hypoxia-directed treatments can be implemented and treatments that are oxygen dependent can be avoided. Contrary to expectations, there is now abundant evidence that tumor hypoxia does not correlate with tumor size, grade, and extent of necrosis or blood hemoglobin status [57–62]. Moreover, most of the commonly used clinicopathologic parameters for evaluation of tumor hypoxia are not strong indicators of prognosis.

Methods to evaluate tumor hypoxia

Tumor oxygenation has been evaluated by several methods and tumor hypoxia to predicted patient outcome in cancers of the uterine cervix [63], lung [59], head and neck [64–67], and glioma (Fig. 6) [68,69]. Most of these studies, however, have shown widespread heterogeneity in tumor hypoxia within a tumor, between tumors, and between patients with the same tumor type [70]. Although hypoxia generally resolves when a tumor shrinks after treatment with either radiotherapy or chemotherapy, it may show paradoxical results in some tumors, perhaps because of hypoxic cell sparing by the treatment (Fig. 7).

Currently available assays for tumor hypoxia can be categorized as in vivo (invasive and noninvasive) or ex vivo (invasive) biopsy [5,71,72]. A useful assay must distinguish normoxic regions from ones that are hypoxic at a level relevant to cancer, P_{O_2} in the 5 mm Hg range. Experience has shown that regional levels of hypoxia should be measured for individual patients and tumor sites. To be maximally successful, hypoxia-directed imaging and treatment should target both chronic hypoxia and hypoxia resulting from transient interruption of blood flow (Fig. 8) [73]. The assay should reflect intracellular P_{O_2} rather than blood flow or some consequence of O_2 on subsequent biochemistry. The observed temporal heterogeneity in tissue P_{O_2} suggests that a secondary effect, such as intracellular redox status, is not as relevant to cancer

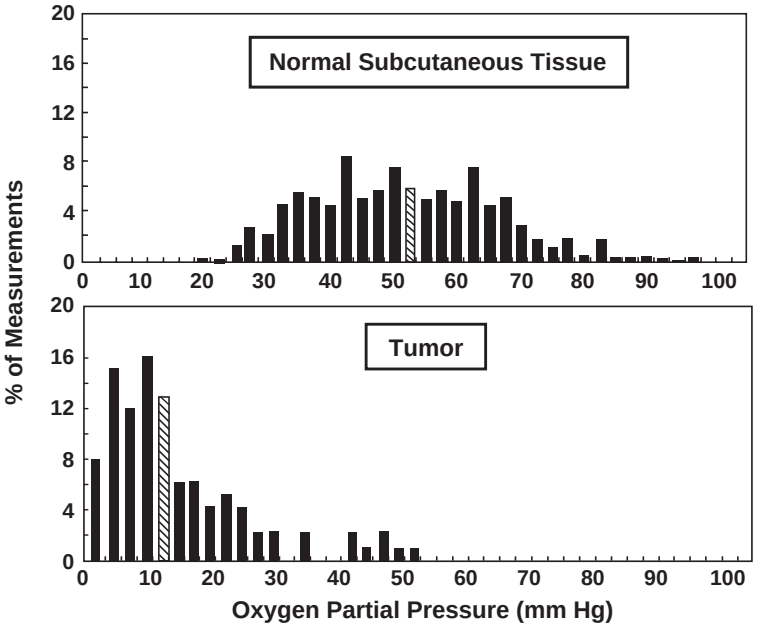

Fig. 6. Oxygen distribution in a metastatic lymph node from a primary head and neck cancer and surrounding normal tissue. These measurements were made with Eppendorf oxygen electrode in a single patient. The median values are represented by hashed bars (*From* Adam M, Gabalski EC, Bloch DA, Ochlert JW, Brown JM, Elsaid AA, et al. Tissue oxygen distribution in head and neck cancer patients. Head Neck 1999;21:146–53; and Brown JM. The hypoxic cell: a target for selective cancer therapy. Eighteenth Bruce F. Cain Memorial Award lecture. Cancer Res 1999;59:5864; with permission.)

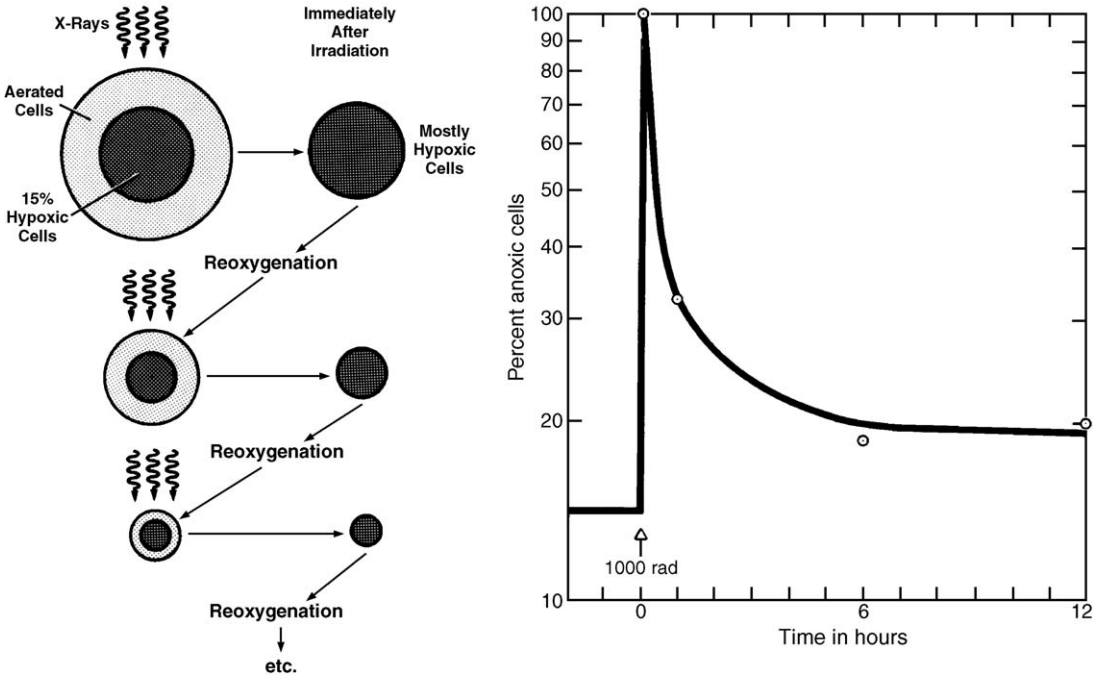

Fig. 7. Reoxygenation in a tumor containing a mixture of aerated and hypoxic cells. This illustrates the changes with each successive fraction of radiation and the sensitivity of oxygenated cells to radiation. (*From* Hall EJ. Radiobiology for the radiologist. Philadelphia: Lippincott Williams & Wilkins; 2000. p. 146–7; with permission.)

treatment outcome as the intracellular partial pressure of O_2. Other desirable characteristics for an ideal clinical hypoxia assay include (1) simple and noninvasive method, (2) nontoxic, (3) rapid and easy to perform with consistency between laboratories, and (4) the ability to quantify without the need for substantial calibration of the detection instrumentation. Location of the tumor in a patient should not be a limiting factor for the assay. Lastly, spatial heterogeneity in the distribution of hypoxia dictates that the ideal assay must provide a complete locoregional evaluation of the tumor. All of these requirements suggest an important role for imaging in evaluating hypoxia.

Polarographic electrode measurements

Early experience evaluating oxygenation of tumors is largely based on direct measurement of O_2 levels using very fine polarographic oxygen electrodes. This assay can be calibrated in units of millimeters of mercury and has been referred to as a gold standard. Heterogeneity of hypoxia within a tumor, which shows a gradient toward the center of the tumor, poses a difficulty for accurately mapping regional Po_2 by this method [58,74]. The electrodes do not provide full maps of a tumor area; they only provide a histogram of the distribution of cell regions as a function of the electrode's reading. There may also be interlaboratory variations in calibration of the electrodes [75]. Polarographic electrodes measure oxygen tension in a group of cells and the readings can be influenced by the presence of blood [76].

Although image-guided sampling can be used to select the path and depth of electrode deployment to avoid blood vessels [77], anatomic imaging methods are notoriously limited in identifying areas of viable tissue within a tumor. Hypodense areas visualized within a tumor on CT (considered necrotic) can indeed have measurable levels of oxygen [76]. Selection of close entry points can reduce sampling error [75], but it also might compromise patient compliance. In addition, electrode measurements are limited by the need for accessible tumor location and difficulties with serial measurements. An accurate value of Po_2 may be less informative than once expected, because cells have different respiratory demand and may not exhibit hypoxic responses at

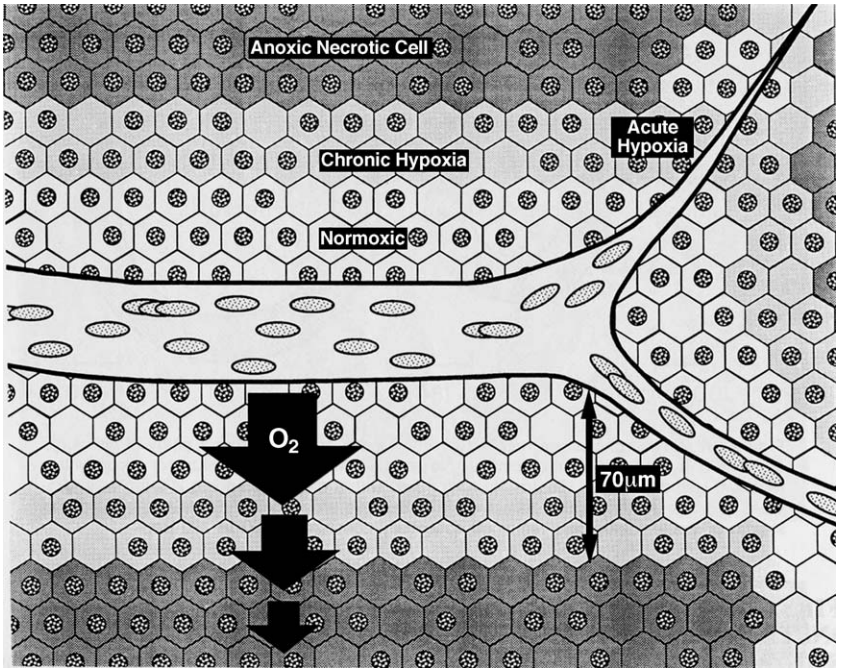

Fig. 8. This diagram illustrates the existence of chronic and acute hypoxia. The former is a result of compromised diffusion of oxygen in actively respiring cells, whereas the latter is a result of acute and temporary blockage of blood vessels in a tumor. (*From* Hall EJ. Radiobiology for the radiologist. Philadelphia: Lippincott Williams & Wilkins; 2000. p. 142; with permission.)

the same levels of tissue oxygenation. Normal cells (eg, cardiomyocytes) experience a level of stress at relatively high Po_2 [78]. Electrode studies commonly report the percentage of readings that fall below some cutoff value that may range from 2.5 to 10 mm Hg, depending on the tumor site. This fractional distribution is a more robust prognostic parameter than absolute Po_2, which is dependent on tissue type and sampling technique, including calibration of the electrode. Also, O_2 is consumed during the electrode assay. The benefit of an absolute value for Po_2 may be less useful and less robust than accurate assessment of the fraction of cells that are hypoxic. For example, it is apparent from Fig. 9 that the distribution of electrode measurements in this tumor is bimodal. The fraction of cells in the hypoxic peak may be much more important than the mean Po_2 or the Po_2 for the nadir separating hypoxia and normoxia. These limitations prompted the search for a noninvasive method that could be done serially to characterize and quantify hypoxia in cancer patients. Imaging methods for hypoxia provide a complete anatomic map of relative oxygenation level in tumor regions with good spatial resolution and in an environment that tends to be highly heterogeneous.

Evaluating angiogenesis

Angiogenesis can be evaluated by either direct or indirect methods. Direct methods were started with largely fluorescent techniques, such as intravital fluorescent video microscopy [79], fluorophore coupling of fibronectin, quenched near-infrared fluorochromes to matrix metalloproteinase-2 substrates, MR imaging [10,80], and color Doppler vascularity index [81–83]. The simplicity of dynamic contrast-enhanced MR imaging has led to fairly widespread use of this technique [84]. It provides a signal that effectively integrates vascular blood flow, blood volume, and vascular permeability.

Noninvasive imaging of the $\alpha_V\beta_3$ integrins that are abundant on vascular endothelium has been attempted by investigators using MR imaging [85], ultrasound [86,87], PET [88–91], and endostatins [92]. The $\alpha_V\beta_3$ integrin is a transmembrane cell adhesion receptor that leads to tumor cells binding of extracellular matrix proteins. The receptor is highly expressed on activated endothelial cells but only weakly expressed in mature endothelium. This has led to $\alpha_V\beta_3$ integrin being evaluated as a target for tumor-specific therapy. The arginine–glycine–

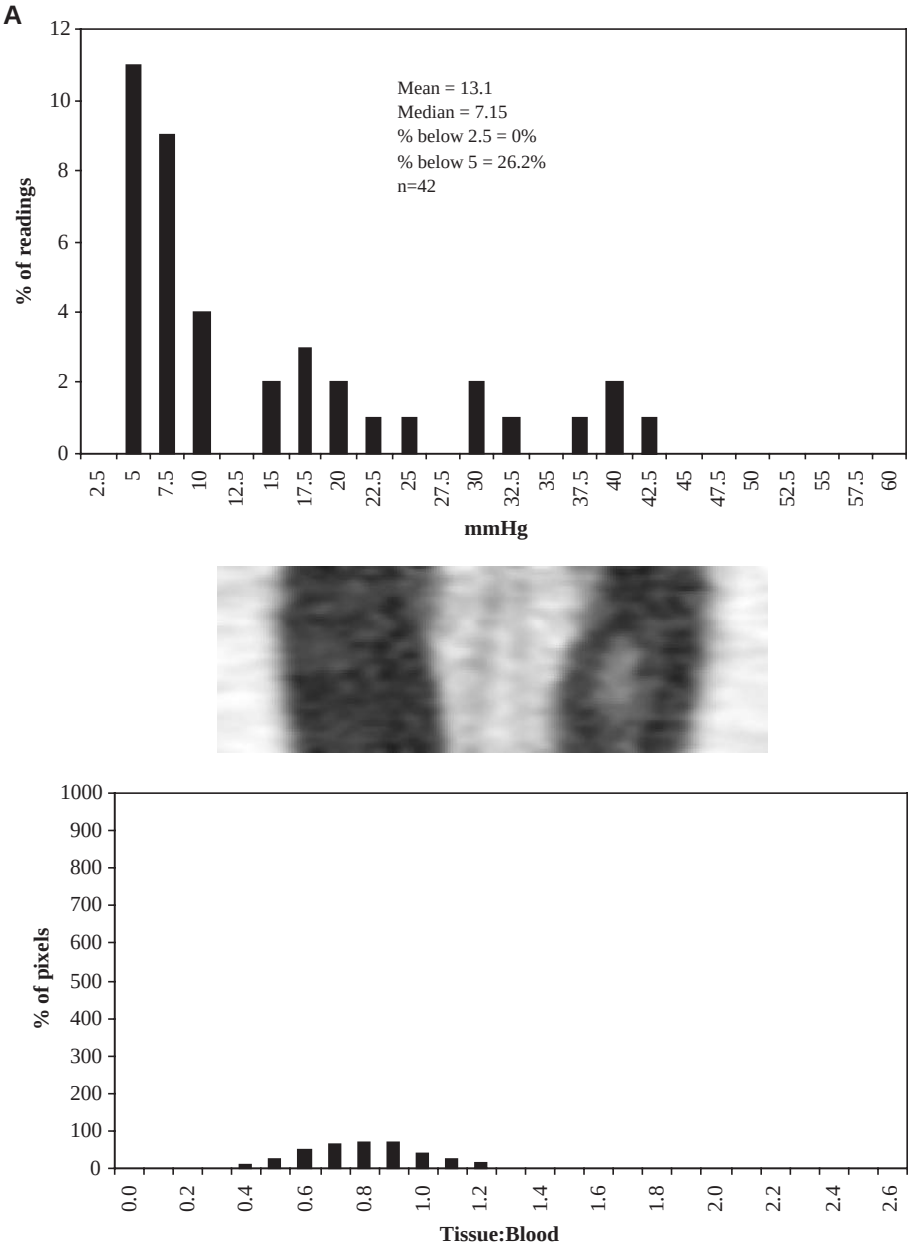

Fig. 9. Comparison of oxygen electrode measurements in a patient with liposarcoma (*A*) and another with osteosarcoma (*B*). Histogram of oxygen electrode Po_2 measurements (*top*), coronal slice of FMISO image (*center*), and tissue:blood histogram of the FMISO uptake into the tumor (*bottom*).

aspartic acid tripeptide recognizes the $\alpha_V\beta_3$ receptor, although it cross-reacts with other integrins. A labeled arginine–glycine–aspartic acid-containing glycopeptide shows great promise as an imaging agent and has also been suggested as a potential therapeutic agent [88–90].

PET and hypoxia imaging

Hypoxia imaging presents the special challenge of making a positive image out of low levels of O_2. Chemists have developed two different imaging agents to address this problem: bioreductive alkyl-

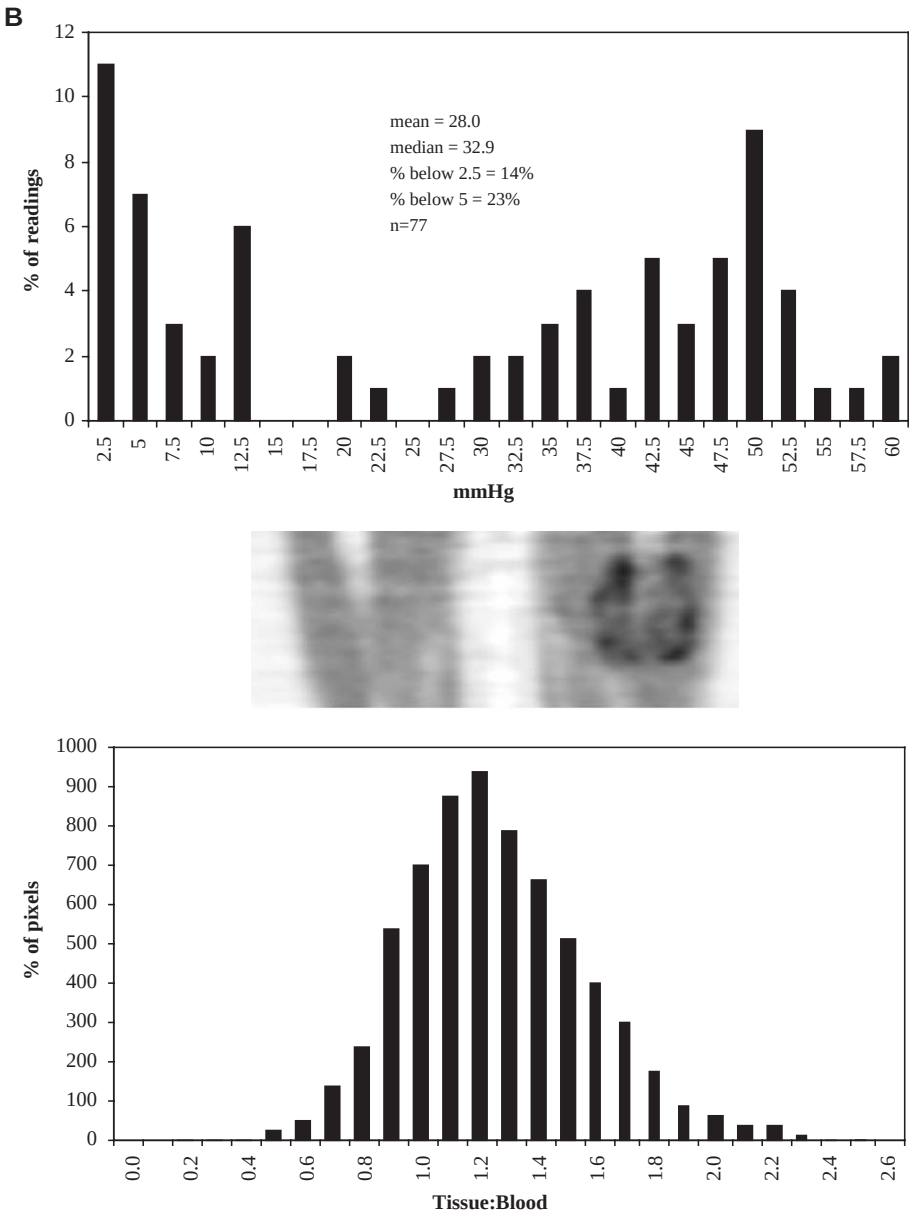

Fig. 9 (*continued*).

ating agents that are O_2-sensitive and metal chelates that are sensitive to the intracellular redox state that develops as a consequence of hypoxia.

Nitroimidazole compounds

Misonidazole, an azomycin-based hypoxic cell sensitizer introduced in clinical radiation oncology nearly three decades ago, binds covalently to intracellular molecules at levels that are inversely proportional to intracellular oxygen concentration below about 10 mm Hg. It is a lipophilic 2-nitroimidazole derivative whose uptake in hypoxic cells is dependent on the sequential reduction of the nitro group on the imidazole ring [93]. This mechanism requires that the cell be alive and undergoing electron transport to provide the electron that initiates the bioreduction

step. In the absence of electron transport, the tracer is not reduced and not accumulated. The one-electron reduction product is an unstable radical anion that either gives up its extra electron to O_2 or picks up a second electron. In the presence of O_2, the nitroimidazole simply goes through a futile reduction cycle and is returned to its initial state. In the absence of an alternative electron acceptor, the nitroimidazole continues to accumulate electrons to form the hydroxylamine alkylating agent and become trapped within the alive but O_2-deficient cell (Fig. 10). This unique biochemical mechanism leads to a tracer whose uptake is inversely related to the oxygen tension within the cell. If cells are reoxygenated and then exposed to a new batch of the tracer, it is not accumulated.

[^{18}F]-fluoromisonidazole (FMISO) is an imaging agent derived from misonidazole, one of the earliest radiosensitizers used in clinical radiation therapy. It has a high hypoxia-specific factor, defined as the ratio of uptake in hypoxic cells compared with normoxic cells, which determines the uptake and specificity in vitro. For FMISO the hypoxia-specific factor is between 20 and 50 [94] and is proportional to the magnitude of hypoxic fraction measured by a survival assay. Prodrug imaging agents, such as FMISO, are bioreductively activated in hypoxic tissue but the process is inhibited by the presence of oxygen in tissues. The result is a positive image of the absence of O_2.

FMISO is a highly stable and robust radiopharmaceutical that can be used to quantify tissue hypoxia using PET technology [60,95]. Its easy synthesis and optimal safety profile are responsible for its ready acceptance in the clinic. After extensive clinical validation, FMISO remains the most commonly used agent for hypoxia PET imaging [59,60,96–101]. Its biodistribution and dosimetry characteristics are ideal for PET imaging [102]. The partition coefficient of FMISO is 0.41 [103], similar to that of the blood flow agent antipyrine, so that initially after injection the tissue distribution reflects blood flow, but after about an hour the distribution reflects its partition coefficient. It is homogeneously distributed with no tissue specificity [78].

The distribution of pixel uptake values after about 90 minutes is narrowly dispersed. This has led to a simple analysis of FMISO PET image by scaling the pixel uptake to plasma concentration. The mean value for this ratio in all tissues is close to unity and almost all normoxic pixels have a value of less than 1.2. The magnitude of the intermediate radical anion product parallels nitroreductase levels, which vary only slightly, so this factor does not affect the imaging analysis of fractional hypoxic volume [96]. The optimum time for imaging seems to be between 90 and 120 minutes and can be adjusted to fit the clinic schedule so that, to the patient or the imaging technologist, the procedure is very similar to a bone scan. Although the tumor:background ratio does not show high contrast, this does not compromise image interpretation. Hypoxia images can be interpreted qualitatively or quantitatively. Qualitative interpretations have been used with a scoring system to grade the uptake in a tumor vis-à-vis normal tissue [56]. After extensive validation studies, the authors prefer a simple but accurate quantitation method using a venous blood sample to calculate a tissue:blood ratio [4,104]. The tumor:plasma ratio has proved useful to estimate the degree of hypoxia in a number of studies, as has the tumor:muscle ratio [101]. The FMISO ratio image provides a reliable and reproducible method that can be introduced readily in the clinic.

Fractional hypoxic volume, defined as the proportion of pixels within the imaged tumor volume having a ratio above some cutoff value, has been used

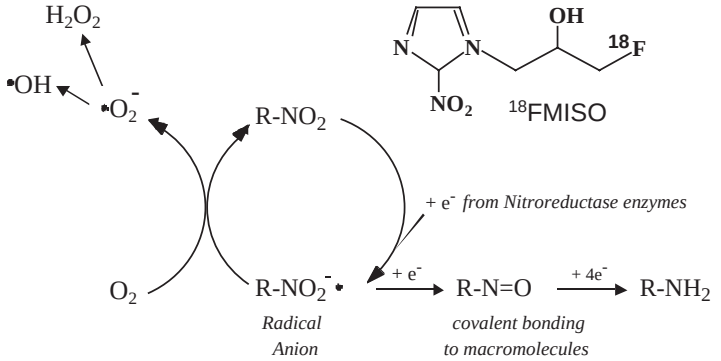

Fig. 10. Structure of misonidazole showing the mechanism of action in the presence and absence of oxygen.

[96] but this requires accurate delineation of tumor margins to define the denominator. The authors prefer the tumor hypoxic volume parameter, which is the total number of pixels with a tissue:blood ratio (T:B) greater than or equal to 1.2. Expressed in milliliters, it is a measure of the extent of tissue hypoxia and obviates the need for stringent demarcation of the tumor boundaries [4]. The advantage of this simple analysis is that it is insensitive to blood flow. It requires only the viability of the hypoxic cell as defined by active electron transport. Mathematic models have been evaluated for more detailed analysis [105], but this level of sophistication is not likely to find a role in routine clinical imaging.

A typical protocol for PET scanning with [^{18}F]-FMISO uses an intravenous administration of a dose of 3.7 mBq (0.1 mCi)/kg, which results in an effective total body dose equivalent of 0.0126 mGy/mBq [102]. Scanning begins after 90 to 120 minutes and lasts for 20 minutes with blood sampling midway during the scan. A transmission scan (20 minutes) is used for attenuation correction of emission data. Typically one axial field of view of 15-cm craniocaudal dimension is acquired. An FDG scan of the same region is routinely obtained for these patients, with care taken to reposition the patients between images. Addition of FDG imaging data increases the sensitivity of FMISO imaging by indicating the full extent of tumor and helps in correlating metabolic activity and hypoxia in tumor (Figs. 10–15) [13].

Alternative azomycin imaging agents

To improve image contrast, some groups have developed alternative azomycin radiopharmaceuticals for hypoxia imaging by attempting to manipulate the rate of blood clearance [106–108]. Elongation factor-1 was initially developed because of the availability of an antibody stain to verify the distribution in tissue samples [109]. Fluoroerythronitroimidazole was developed as a more hydrophilic derivative of misonidazole that might have more rapid plasma clearance and this could be an imaging advantage. Fluoroetanidazole has binding characteristics similar to FMISO, but has been reported to have less retention in liver and fewer metabolites in animals [110], but the advantages were not sufficient to carry these derivatives to wide clinical testing. Single-photon emission CT–based hypoxia imaging compounds have been introduced with the hope of taking this technology to gamma camera imaging [111]. The University of Alberta group pioneered the development of iodinated derivatives of nitroimidazoles. Direct halogenation of the imidazole ring does not lead to a stable radiopharmaceutical, so the general approach has been to place sugar residues between the nitroimidazole and the radioiodine to stabilize the molecule. These products exhibit minimal deiodination and two derivatives have been evaluated in patients. Introduction of the sugar results in a more water-soluble molecule than misonidazole. This has two consequences: the hydrophilic product clears more rapidly, but its clearance and its background distribution in normoxic tissues is dependent on blood flow. The resulting images have higher contrast when imaging is typically initiated 110 minutes after injection. A simple ratio analysis to infer hypoxia, however, as used for FMISO images, is not valid.

The success with radioiodinated azamycin arabinosides led to attempts to develop technetium derivatives of 2-nitroimidazole. The practical advantages of a Tc-99m label are well known in the nuclear medicine community and include ready availability at low cost, convenient half-life for hypoxia measurements, and versatile chemistry. Two different approaches have been evaluated: both BMS181321 and HL91 were synthesized and evaluated as hypoxia-based agents. Although both of these molecules involve ligands with potential hypoxia-specific binding characteristics, the reduction chemistry of the metal core is also subject to redox chemistry that can result in separation of the Tc = O core from the ligand [106,112]. The BMS compound was so lipophilic that its background activity was high, especially in the abdomen. A less lipophilic derivative, BMS194796,

Fig. 11. Corresponding FMISO (*left*) and FDG (*right*) images of a patient with cancer of the larynx with metastatic lymph nodes.

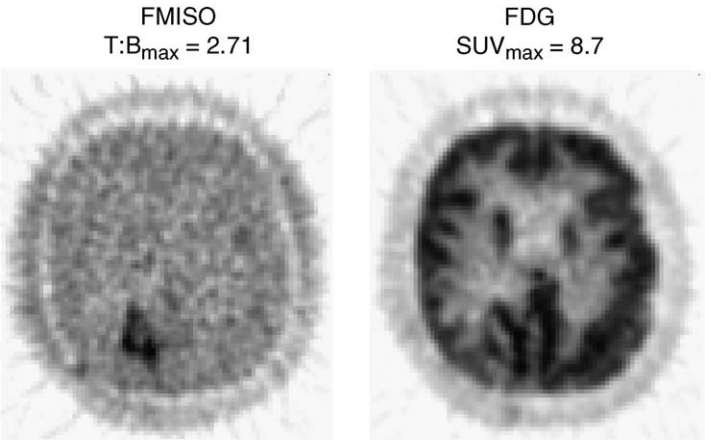

Fig. 12. Corresponding transaxial FMISO (*left*) and FDG (*right*) images of a patient with glioblastoma multiforme in the right occipital region. SUV, standardized uptake value.

has been developed with better clearance properties, especially from the liver [113]. Both of the BMS compounds involve a nitroimidazole group, although it is probably not the dominant influence in determining the biodistribution kinetics of the radiopharmaceutical and its specific localization in hypoxic tissues. The HL91 molecule, TcBnAO, does not include a nitroimidazole; the Tc-ligand coordination chemistry is directly reduced and retained in hypoxic environments [112]. The resulting lack of specificity has led to abandonment of this molecule as a tracer for imaging hypoxia. It also requires a much lower level of O_2 for its reduction and uptake, raising concerns for routine clinical applications [114].

Single-photon emission CT radiopharmaceuticals include both the iodinated compounds (eg, [^{123}I] radioiodinated azamycin arabinosides [115]) and technetium-based agents. These radiopharmaceuticals, in contrast to PET agents, suffer from lower image contrast and less potential for quantification [107]. Furthermore, the absence of a gold standard for hypoxia evaluation complicates validation of all hypoxia markers, including FMISO [94], and treatment outcome studies are urgently needed to provide convincing evidence for the clinical value of hypoxia imaging.

The altered redox environment associated with hypoxia has led to another class of radiopharmaceuticals for imaging hypoxia. Copper bis(thiosemicarbazones) are a class of molecules evaluated as freely diffusible but retained blood flow tracers. The ^{64}Cu-labeled acetyl derivative of pyruvaldehyde bis [N4-methylthiosemicarbazonato] copper (II) complex, Cu-ATSM, has the potential advantage of a longer half-life for practical clinical use [116–118], although the mechanism of retention is less well validated than FMISO. Fujibayashi et al [119] showed that the intracellular retention mechanism was related to the copper-reduction chemistry, Cu^{++} to Cu^{+}, which has a redox potential of −297 mV for Cu-ATSM. Several biologic systems have comparable redox potentials: −315 mV for NADH and −230 mV for glutathione.

Several laboratories showed that Cu-ATSM was retained in hypoxic areas [119]. This radiopharma-

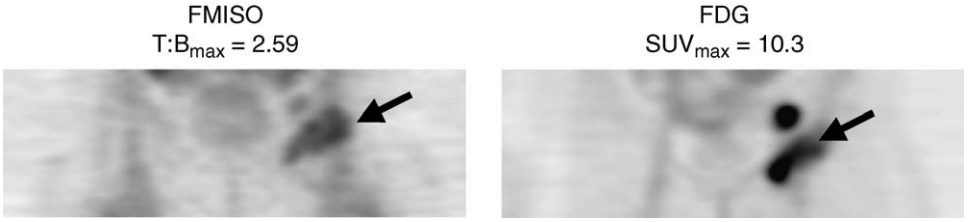

Fig. 13. Corresponding FMISO (*left*) and FDG (*right*) images of a patient with soft tissue sarcoma of the pelvis.

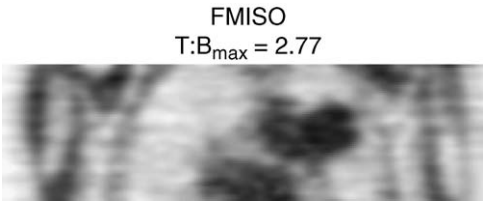

Fig. 14. FMISO image of a patient with a non–small cell lung cancer.

ceutical has rapid washout from normoxic areas. It is a useful imaging agent for identifying regions of tissue that have higher levels of reducing agents, such as NADH, as a consequence of hypoxia. There is ample evidence in the literature that the concentration of NADH is increased under extended hypoxic conditions. This mechanism is distinct from that for the nitroimidazoles, in that the copper agents reflect a consequence of hypoxia rather than the actual Po_2. This mechanistic difference might limit the role of Cu-ATSM for measuring a prompt reoxygenation response because the increased levels of NADH persist. Diffusion of NADH-related reducing equivalents might make Cu-ATSM less reflective of the spatial heterogeneity of hypoxia. The same characteristics make the Cu agents preferable for imaging chronic hypoxia, however, where levels of NADH can increase by several fold. There are several useful radionuclides of copper that can be used for imaging [117,120].

PET imaging is likely to become the dominant method for evaluating tumor hypoxia in patients. It simply stands out as the ideal procedure for evaluating tumor hypoxia repeatedly and noninvasively. It has the advantage of evaluating the entire tumor and regional lymph nodes for a patient at the same time in a snapshot fashion. It is less operator-dependent than polarographic oxygen electrodes. Its noninvasiveness and safety profile make it a convenient tool for the follow-up of patients by providing the ability to do repeat imaging [121]. The main advantage of PET is its ability accurately to quantify tissue uptake of the hypoxia tracer, independent of anatomic location of the tumor. Widespread availability of PET scanners (and now PET/CT scanners) and [^{18}F]-labeled hypoxia tracers in the community make this procedure within reach of every community nuclear medicine center. Although the level of pretherapy hypoxia is an important parameter, its change with treatment gives an even better understanding of the effectiveness of treatment.

Hypoxia imaging can be combined with other indicators of tissue hemodynamics and oxygenation, such as perfusion imaging using [^{15}O]water, and tissue markers of proteomic response to hypoxia, such as vascular density and HIF-1α expression using immunocytochemistry, in a complementary fashion. Recently introduced PET/CT scanners provide the opportunity to combine anatomic imaging and functional information. This will not only increase the accuracy of hypoxia imaging but will also allow the images to be incorporated into radiation treatment planning systems to plan and deliver hypoxic subvolume directed radiotherapy boost effectively using intensity-modulated radiotherapy [54,55,122].

Summary

There is a clear need in cancer treatment for a noninvasive imaging assay that evaluates the oxygenation status and heterogeneity of hypoxia and angiogenesis in individual patients. Such an assay could be used to select alternative treatments and to monitor the effects of treatment. Of the several methods available, each imaging procedure has at least one disadvantage. The limited quantitative potential of single-photon emission CT and MR imaging always limits tracer imaging based on these detection systems. PET imaging with FMISO and Cu-ATSM is ready for coordinated multicenter trials,

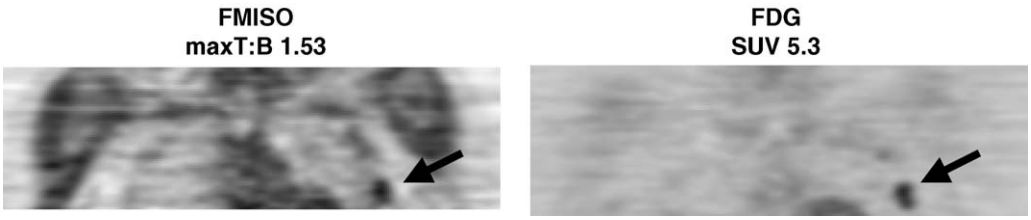

Fig. 15. Corresponding FMISO (*left*) and FDG (*right*) images of a patient with breast cancer.

however, that should move aggressively forward to resolve the debate over the importance of hypoxia in limiting response to cancer therapy. Advances in radiation treatment planning, such as intensity-modulated radiotherapy, provide the ability to customize radiation delivery based on physical conformity [54,55,123,124]. With incorporation of regional biologic information, such as hypoxia and proliferating vascular density in treatment planning, imaging can create a biologic profile of the tumor to direct radiation therapy [124,125]. Presence of widespread hypoxia in the tumor benefits from a systemic hypoxic cell cytotoxin [126]. Angiogenesis is also an important therapeutic target. Imaging hypoxia and angiogenesis complements the efforts in development of antiangiogenesis and hypoxia-targeted drugs. The complementary use of hypoxia and angiogenesis imaging methods should provide the impetus for development and clinical evaluation of novel drugs targeted at angiogenesis and hypoxia [50,127–129]. Hypoxia imaging brings in information different from that of FDG-PET but it will play an important niche role in oncologic imaging in the near future.

FMISO, radioiodinated azamycin arabinosides, and Cu-ATSM are all being evaluated in patients. The Cu-ATSM images show the best contrast early after injection but these images are confounded by blood flow and their mechanism of localization is one step removed from the intracellular O_2 concentration. FMISO has been criticized as inadequate because of its clearance characteristics, but its uptake after 2 hours is probably the most purely reflective of regional Po_2 at the time the radiopharmaceutical is used. The FMISO images show less contrast than those of Cu-ATSM because of the lipophilicity and slower clearance of FMISO but attempts to increase the rate of clearance led to tracers whose distribution is contaminated by blood flow effects. For single-photon emission CT the only option is radioiodinated azamycin arabinosides, because the technetium agents are not yet ready for clinical evaluation. Rather than develop new and improved hypoxia agents, or even quibbling about the pros and cons of alternative agents, the nuclear medicine community needs to convince the oncology community that imaging hypoxia is an important procedure that can lead to improved treatment outcome.

Acknowledgments

The authors appreciate the following individuals for the help they provided. L.M. Peterson, BA, for help with the manuscript, J.F. Eary, MD, for useful critique, and H.S. Vesselle, MD, for help with the oxygen electrode studies.

References

[1] Wahl RL. Anatomolecular imaging with 2-deoxy-2-[18F]fluoro-D-glucose: bench to outpatient center. Mol Imaging Biol 2003;5:49–56.
[2] Herschman HR. Molecular imaging: looking at problems, seeing solutions. Science 2003;302:605–8.
[3] Chapman JD, Bradley JD, Eary JF, Haubner R, Larson SM, Michalski JM, et al. Molecular (functional) imaging for radiotherapy applications: an RTOG symposium. Int J Radiat Oncol Biol Phys 2003;55:294–301.
[4] Rajendran J, Muzi M, Peterson LM, Diaz AZ, Spence AM, Schwartz DS, et al. Analyzing the results of [F-18] FMISO PET hypoxia imaging: what is the best way to quantify hypoxia? J Nucl Med 2002;43:102P.
[5] Peters L, McKay M. Predictive assays: will they ever have a role in the clinic? Int J Radiat Oncol Biol Phys 2001;49:501–4.
[6] Rowland DJ, Lewis JS, Welch MJ. Molecular imaging: the application of small animal positron emission tomography. J Cell Biochem Suppl 2002; 39:110–5.
[7] Maclean D, Northrop JP, Padgett HC, Walsh JC. Drugs and probes: the symbiotic relationship between pharmaceutical discovery and imaging science. Mol Imaging Biol 2003;5:304–11.
[8] Collier TL, Lecomte R, McCarthy TJ, Meikle S, Ruth TJ, Scopinaro F, et al. Assessment of cancer-associated biomarkers by positron emission tomography: advances and challenges. Dis Markers 2002; 18:211–47.
[9] Gambhir SS. Molecular imaging of cancer with positron emission tomography. Nat Rev Cancer 2002;2: 683–93.
[10] Bhujwalla ZM, Artemov D, Aboagye E, Ackerstaff E, Gillies RJ, Natarajan K, et al. The physiological environment in cancer vascularization, invasion and metastasis. Novartis Found Symp 2001;240:23–38 [discussion: 38–45, 152–3].
[11] Thomlinson RH, Gray LH. The histological structure of some human lung cancers and the possible implications for radiotherapy. Br J Cancer 1955;9: 537–49.
[12] Kourkourakis MI, Giotromanolaki A. Cancer vascularization: implications in radiotherapy? Int J Radiat Oncol Biol Phys 2000;48:545–53S.
[13] Rajendran JG, O'Sullivan F, Peterson LM, Schwartz DL, Conrad EU, Spence AM, et al. Hypoxia and glucose metabolism in malignant tumors: evaluation by FMISO and FDG PET imaging. Clin Cancer Res 2004;10:2245–52.
[14] Scandurro AB, Weldon CW, Figueroa YG, Alam J, Beckman BS. Gene microarray analysis reveals a

novel hypoxia signal transduction pathway in human hepatocellular carcinoma cells. Int J Oncol 2001; 19:129–35.
[15] Villaret DB, Wang T, Dillon D, Xu J, Sivam D, Cheever MA, et al. Identification of genes overexpressed in head and neck squamous cell carcinoma using a combination of complementary DNA subtraction and microarray analysis. Laryngoscope 2000; 110:374–81.
[16] Agani F, Semenza GL. Mersalyl is a novel inducer of vascular endothelial growth factor gene expression and hypoxia-inducible factor 1 activity. Mol Pharmacol 1998;54:749–54.
[17] Bae MK, Kwon YW, Kim MS, Bae SK, Bae MH, Lee YM, et al. Identification of genes differentially expressed by hypoxia in hepatocellular carcinoma cells. Biochem Biophys Res Commun 1998;243:158–62.
[18] Dachs GU, Tozer GM. Hypoxia modulated gene expression: angiogenesis, metastasis and therapeutic exploitation. Eur J Cancer 2000;36:1649–60.
[19] Eisma RJ, Spiro JD, Kreutzer DL. Vascular endothelial growth factor expression in head and neck squamous cell carcinoma. Am J Surg 1997;174:513–7.
[20] Hockel M, Schlenger K, Hockel S, Vaupel P. Hypoxic cervical cancers with low apoptotic index are highly aggressive. Cancer Res 1999;59:4525–8.
[21] Guillemin K, Krasnow MA. The hypoxic response: huffing and HIFing. Cell 1997;89:9–12.
[22] Jiang BH, Semenza GL, Bauer C, Marti HH. Hypoxia-inducible factor 1 levels vary exponentially over a physiologically relevant range of O_2 tension. Am J Physiol 1996;271:C1172–80.
[23] Clavo AC, Wahl RL. Effects of hypoxia on the uptake of tritiated thymidine, L-leucine, L-methionine and FDG in cultured cancer cells. J Nucl Med 1996;37: 502–6.
[24] Burgman P, Odonoghue JA, Humm JL, Ling CC. Hypoxia-induced increase in FDG uptake in MCF7 cells. J Nucl Med 2001;42:170–5.
[25] Ivan M, Kondo K, Yang H, Kim W, Valiando J, Ohh M, et al. HIFalpha targeted for VHL-mediated destruction by proline hydroxylation: implications for O_2 sensing. Science 2001;292:464–8.
[26] Huang LE, Arany Z, Livingston DM, Bunn HF. Activation of hypoxia-inducible transcription factor depends primarily upon redox-sensitive stabilization of its alpha subunit. J Biol Chem 1996;271:32253–9.
[27] Bos R, Zhong H, Hanrahan CF, Mommers EC, Semenza GL, Pinedo HM, et al. Levels of hypoxia-inducible factor-1 alpha during breast carcinogenesis. J Natl Cancer Inst 2001;93:309–14.
[28] Zhong H, De Marzo AM, Laughner E, Lim M, Hilton DA, Zagzag D, et al. Overexpression of hypoxia-inducible factor 1alpha in common human cancers and their metastases. Cancer Res 1999;59: 5830–5.
[29] Marxsen JH, Schmitt O, Metzen E, Jelkmann W, Hellwig-Burgel T. Vascular endothelial growth factor gene expression in the human breast cancer cell line MX-1 is controlled by O_2 availability in vitro and in vivo. Ann Anat 2001;183:243–9.
[30] Yaziji H, Gown AM. Immunohistochemical analysis of gynecologic tumors. Int J Gynecol Pathol 2001; 20:64–78.
[31] Folkman J. Tumor angiogenesis: therapeutic implications. N Engl J Med 1971;285:1182–6.
[32] Gullino PM. Angiogenesis and neoplasia. N Engl J Med 1981;305:884–5.
[33] Hood JD, Cheresh DA. Role of integrins in cell invasion and migration. Nat Rev Cancer 2002;2:91–100.
[34] McDonald DM, Teicher BA, Stetler-Stevenson W, Ng SS, Figg WD, Folkman J, et al. Report from the Society for Biological Therapy and Vascular Biology Faculty of the NCI Workshop on Angiogenesis Monitoring. J Immunother 2004;27:161–75.
[35] Costouros NG, Diehn FE, Libutti SK. Molecular imaging of tumor angiogenesis. J Cell Biochem Suppl 2002;39:72–8.
[36] Weber WA, Haubner R, Vabuliene E, Kuhnast B, Wester HJ, Schwaiger M. Tumor angiogenesis targeting using imaging agents. Q J Nucl Med 2001; 45:179–82.
[37] Koukourakis MI, Giatromanolaki A, Sivridis E, Fezoulidis I. Cancer vascularization: implications in radiotherapy? Int J Radiat Oncol Biol Phys 2000; 48:545–53.
[38] Jain RK, Safabakhsh N, Sckell A, Chen Y, Jiang P, Benjamin L, et al. Endothelial cell death, angiogenesis, and microvascular function after castration in an androgen-dependent tumor: role of vascular endothelial growth factor. Proc Natl Acad Sci U S A 1998;95:10820–5.
[39] Hall EJ. Radiobiology for the radiologist. Philadelphia: Lippincott Williams & Wilkins; 2000.
[40] Marples B, Greco O, Joiner MC, Scott SD. Molecular approaches to chemo-radiotherapy. Eur J Cancer 2002;38:231–9.
[41] Overgaard J, Horsman MR. Modification of hypoxia-induced radioresistance in tumors by the use of oxygen and sensitizers. Semin Radiat Oncol 1996;6: 10–21.
[42] Fowler JF. Eighth annual Juan del Regato lecture. Chemical modifiers of radiosensitivity–theory and reality: a review. Int J Radiat Oncol Biol Phys 1985; 11:665–74.
[43] Frommhold H, Guttenberger R, Henke M. The impact of blood hemoglobin content on the outcome of radiotherapy. The Freiburg experience. Strahlenther Onkol 1998;174(Suppl 4):31–4.
[44] Evans SM, Koch CJ. Prognostic significance of tumor oxygenation in humans. Cancer Lett 2003;195:1–16.
[45] Koong AC, Denko NC, Hudson KM, Schindler C, Swiersz L, Koch C, et al. Candidate genes for the hypoxic tumor phenotype. Cancer Res 2000;60: 883–7.
[46] Blancher C, Moore JW, Talks KL, Houlbrook S, Harris AL. Relationship of hypoxia-inducible factor (HIF)-1alpha and HIF-2alpha expression to vascular

endothelial growth factor induction and hypoxia survival in human breast cancer cell lines. Cancer Res 2000;60:7106–13.
[47] Sutherland RM. Tumor hypoxia and gene expression: implications for malignant progression and therapy. Acta Oncol 1998;37:567–74.
[48] Amellem O, Pettersen EO. Cell inactivation and cell cycle inhibition as induced by extreme hypoxia: the possible role of cell cycle arrest as a protection against hypoxia-induced lethal damage. Cell Prolif 1991;24:127–41.
[49] Moulder JE, Rockwell S. Tumor hypoxia: its impact on cancer therapy. Cancer Metastasis Rev 1987;5: 313–41.
[50] Blancher C, Harris AL. The molecular basis of the hypoxia response pathway: tumour hypoxia as a therapy target. Cancer Metastasis Rev 1998;17:187–94.
[51] Brown JM. Exploiting the hypoxic cancer cell: mechanisms and therapeutic strategies. Mol Med Today 2000;6:157–62.
[52] Lee DJ, Moini M, Giuliano J, Westra WH. Hypoxic sensitizer and cytotoxin for head and neck cancer. Ann Acad Med Singapore 1996;25:397–404.
[53] Sartorelli AC, Hodnick WF. Mitomycin C: a prototype bioreductive agent. Oncol Res 1994;6:501–8.
[54] Rajendran JG, Schwartz DL, Kinahan PE, Cheng P, Hummel SM, Lewellen B, et al. Imaging with F-18 FMISO-PET permits hypoxia directed radiotherapy dose escalation for head and neck cancer. J Nucl Med 2003;44:415, 127P.
[55] Chao KS, Bosch WR, Mutic S, Lewis JS, Dehdashti F, Mintun MA, et al. A novel approach to overcome hypoxic tumor resistance: Cu-ATSM-guided intensity-modulated radiation therapy. Int J Radiat Oncol Biol Phys 2001;49:1171–82.
[56] Rischin D, Peters L, Hicks R, Hughes P, Fisher R, Hart R, et al. Phase I trial of concurrent tirapazamine, cisplatin, and radiotherapy in patients with advanced head and neck cancer. J Clin Oncol 2001; 19:535–42.
[57] Brown MJ. The hypoxic cell: a target for selective cancer therapy. Eighteenth Bruce F. Cain memorial award lecture. Cancer Res 1999;59:5863–70.
[58] Hockel M, Schlenger K, Knoop C, Vaupel P. Oxygenation of carcinoma of the uterine cervix: evaluation by computerized oxygen tension measurements. Cancer Res 1991;51:6098–102.
[59] Koh WJ, Bergman KS, Rasey JS, Peterson LM, Evans ML, Graham MM, et al. Evaluation of oxygenation status during fractionated radiotherapy in human non small cell lung cancers using [F-18]fluoromisonidazole positron emission tomography. Int J Radiat Oncol Biol Phys 1995;33:391–8.
[60] Rajendran JG, Wilson D, Conrad EU, Peterson LM, Bruckner JD, Rasey JS, et al. F-18 FMISO and F-18 FDG PET imaging in soft tissue sarcomas: correlation of hypoxia, metabolism and VEGF expression. Eur J Nucl Med 2003;30:695–704.
[61] Rajendran JG, Peterson LM, Schwartz DL, Scharnhrost J, Conrad EU, Grierson JR, et al. F-18 FMISO PET tumor hypoxia imaging: investigating the tumor volume-hypoxia connection. J Nucl Med 2003;44: 1340, 1376P.
[62] Adam M, Gabalski EC, Bloch DA, Ochlert JW, Brown JM, Elsaid AA, et al. Tissue oxygen distribution in head and neck cancer patients. Head Neck 1999;21:146–53.
[63] Hockel M, Schlenger K, Knoop C, Vaupel P. Oxygenation of carcinomas of the uterine cervix: evaluation by computerized O_2 tension measurements. Cancer Res 1991;51:6098–102.
[64] Brizel DM, Sibley GS, Prosnitz LR, Scher RL, Dewhirst MW. Tumor hypoxia adversely affects the prognosis of carcinoma of the head and neck. Int J Radiat Oncol Biol Phys 1997;38:285–9.
[65] Lartigau E, Lusinchi A, Weeger P, Wibault P, Luboinski B, Eschwege F, et al. Variations in tumour oxygen tension (Po_2) during accelerated radiotherapy of head and neck carcinoma. Eur J Cancer 1998;34: 856–61.
[66] Nordsmark M, Overgaard M, Overgaard J. Pretreatment oxygenation predicts radiation response in advanced squamous cell carcinoma of the head and neck. Radiother Oncol 1996;41:31–9.
[67] Ng P, Peterson LM, Schwartz DL, Scharnhrost J, Krohn KA. Can F-18 fluoromisonidazole PET imaging predict treatment response in head and neck cancer? J Nucl Med 2003;44:416, 128P.
[68] Muzi M, Spence AM, Rajendran JG, Grierson JR, Krohn KA. Glioma patients assessed with FMISO and FDG: two tracers provide different Information. J Nucl Med 2003;44:878, 243P.
[69] Valk P, Mathis C, Prados M, Gilbert J, Budinger T. Hypoxia in human gliomas: demonstration by PET with flouorine-18-fluoromisonidazole. J Nucl Med 1992;33:2133–7.
[70] Rajendran J, Lanell P, Schwartz DS, Muzi M, Scharnhorst JD, Eary JF, et al. [F-18] FMISO PET hypoxia imaging in head and neck cancer: heterogeneity in hypoxia - primary tumor vs lymph nodal metastases. J Nucl Med 2002;43:73P.
[71] Stone HB, Brown JM, Phillips TL, Sutherland RM. Oxygen in human tumors: correlations between methods of measurement and response to therapy. Summary of a workshop held November 19–20, 1992, at the National Cancer Institute, Bethesda, Maryland. Radiat Res 1993;136:422–34.
[72] Hockel M, Vaupel P. Tumor hypoxia: definitions and current clinical, biologic, and molecular aspects. J Natl Cancer Inst 2001;93:266–76.
[73] Rasey JS, Casciari JJ, Hofstrand PD, Muzi M, Graham MM, Chin LK. Determining hypoxic fraction in a rat glioma by uptake of radiolabeled fluoromisonidazole. Radiat Res 2000;153:84–92.
[74] Vaupel P, Kelleher DK, Hockel M. Oxygen status of malignant tumors: pathogenesis of hypoxia and significance for tumor therapy. Semin Oncol 2001;28: 29–35.
[75] Nozue M, Lee I, Yuan F, et al. Interlaboratory

variation in oxygen tension measurement by eppendorf "histograph" and comparison with hypoxic marker. J Surg Oncol 1997;66:30–8.
[76] Lartigau E, Le Ridant AM, Lambin P, Weeger P, Martin L, Sigal R, et al. Oxygenation of head and neck tumors. Cancer 1993;71:2319–25.
[77] Brizel DM, Rosner GL, Harrelson J, Prosnitz LR, Dewhirst MW. Pretreatment oxygenation profiles of human soft tissue sarcomas. Int J Radiat Oncol Biol Phys 1994;30:635–42.
[78] Martin GV, Caldwell JH, Graham MM, Grierson JR, Kroll K, Cowan MJ, et al. Noninvasive detection of hypoxic myocardium using fluorine-18-fluoromisonidazole and positron emission tomography. J Nucl Med 1992;33:2202–8.
[79] Jain RK. Angiogenesis and lymphangiogenesis in tumors: insights from intravital microscopy. Cold Spring Harb Symp Quant Biol 2002;67:239–48.
[80] Brasch RC, Li KC, Husband JE, Keogan MT, Neeman M, Padhani AR, et al. In vivo monitoring of tumor angiogenesis with MR imaging. Acad Radiol 2000;7:812–23.
[81] Chen CN, Cheng YM, Lin MT, Hsieh FJ, Lee PH, Chang KJ. Association of color Doppler vascularity index and microvessel density with survival in patients with gastric cancer. Ann Surg 2002;235:512–8.
[82] Cheng WF, Lee CN, Chu JS, Chen CA, Chen TM, Shau WY, et al. Vascularity index as a novel parameter for the in vivo assessment of angiogenesis in patients with cervical carcinoma. Cancer 1999;85:651–7.
[83] Cheng WF, Chen TM, Chen CA, Wu CC, Huang KT, Hsieh CY, et al. Clinical application of intratumoral blood flow study in patients with endometrial carcinoma. Cancer 1998;82:1881–6.
[84] Stevenson JP, Rosen M, Sun W, Gallagher M, Haller DG, Vaughn D, et al. Phase I trial of the antivascular agent combretastatin A4 phosphate on a 5-day schedule to patients with cancer: magnetic resonance imaging evidence for altered tumor blood flow. J Clin Oncol 2003;21:4428–38.
[85] Sipkins DA, Cheresh DA, Kazemi MR, Nevin LM, Bednarski MD, Li KC. Detection of tumor angiogenesis in vivo by alphaVbeta3-targeted magnetic resonance imaging. Nat Med 1998;4:623–6.
[86] Leong-Poi H, Christiansen JP, Klibanov AL, Kaul S, Lindner JR. Noninvasive assessment of angiogenesis by contrast ultrasound imaging with microbubbles targeted to alpha-V integrins. J Am Coll Cardiol 2003;41:430–1.
[87] Leong-Poi H, Christiansen J, Klibanov AL, Kaul S, Lindner JR. Noninvasive assessment of angiogenesis by ultrasound and microbubbles targeted to alpha(v)-integrins. Circulation 2003;107:455–60.
[88] Haubner R, Wester HJ, Weber WA, Mang C, Ziegler SI, Goodman SL, et al. Noninvasive imaging of alpha(v)beta3 integrin expression using 18F-labeled RGD-containing glycopeptide and positron emission tomography. Cancer Res 2001;61:1781–5.
[89] Haubner R, Wester HJ, Burkhart F, Senekowitsch-Schmidtke R, Weber W, Goodman SL, et al. Glycosylated RGD-containing peptides: tracer for tumor targeting and angiogenesis imaging with improved biokinetics. J Nucl Med 2001;42:326–36.
[90] Ogawa M, Hatano K, Oishi S, Kawasumi Y, Fujii N, Kawaguchi M, et al. Direct electrophilic radiofluorination of a cyclic RGD peptide for in vivo alpha(v)-beta3 integrin related tumor imaging. Nucl Med Biol 2003;30:1–9.
[91] Blankenberg FG, Eckelman WC, Strauss HW, Welch MJ, Alavi A, Anderson C, et al. Role of radionuclide imaging in trials of antiangiogenic therapy. Acad Radiol 2000;7:851–67.
[92] Barthel H. Endostatin imaging to help understanding of antiangiogenic drugs. Lancet Oncol 2002;3:520.
[93] Prekeges JL, Rasey JS, Grunbaum Z, Krohn KH. Reduction of fluoromisonidazole, a new imaging agent for hypoxia. Biochem Pharmacol 1991;42: 2387–95.
[94] Chapman JD, Engelhardt EL, Stobbe CC, Schneider RF, Hanks GE. Measuring hypoxia and predicting tumor radioresistance with nuclear medicine assays. Radiother Oncol 1998;46:229–37.
[95] Grierson JR, Link JM, Mathis CA, Rasey JS, Krohn KA. Radiosynthesis of fluorine-18 fluoromisonidazole. J Nucl Med 1989;30:343–50.
[96] Rasey JS, Wui-Jin K, Evans ML, Peterson LM, Lewellen TK, Graham MM, et al. Quantifying regional hypoxia in human tumors with positron emission tomography of [18F]fluoromisonidazole: a pretherapy study of 37 patients. Int J Radiat Oncol Biol Phys 1996;36:417–28.
[97] Rajendran J, Lanell P, Schwartz DS, Scharnhorst JD, Koh WJ, Eary JF, et al. PET imaging in head and neck cancer with [F-18]FMISO and [F-18] FDG: evaluating different aspects of tumor biology - hypoxia and metabolism. Proc Am Assoc Cancer Res 2002;43:758P.
[98] Liu RS, Chu LS, Yen SH, Chang CP, Chou KL, Wu LC, et al. Detection of anaerobic odontogenic infections by fluorine-18 fluoromisonidazole. Eur J Nucl Med 1996;23:1384–7.
[99] Bentzen L, Keiding S, Horsman MR, Falborg L, Hansen SB, Overgaard J. Feasibility of detecting hypoxia in experimental mouse tumours with 18F-fluorinated tracers and positron emission tomography: a study evaluating [18F]Fluoro-2-deoxy-D-glucose. Acta Oncol 2000;39:629–37.
[100] Read SJ, Hirano T, Abbott DF, Sachinidis JI, Tochon-Danguy HJ, Chan JG, et al. Identifying hypoxic tissue after acute ischemic stroke using PET and 18F-fluoromisonidazole. Neurology 1998;51:1617–21.
[101] Yeh SH, Liu RS, Wu LC, Yang DJ, Yen SH, Chang CW, et al. Fluorine-18 fluoromisonidazole tumour to muscle retention ratio for the detection of hypoxia in nasopharyngeal carcinoma. Eur J Nucl Med 1996; 23:1378–83.
[102] Graham MM, Peterson LM, Link JM, Evans ML, Rasey JS, Koh WJ, et al. Fluorine-18-fluoromisoni-

dazole radiation dosimetry in imaging studies. J Nucl Med 1997;38:1631–6.
[103] Rasey JS, Koh WJ, Grierson JR, Grunbaum Z, Krohn KA. Radiolabelled fluoromisonidazole as an imaging agent for tumor hypoxia. Int J Radiat Oncol Biol Phys 1989;17:985–91.
[104] Koh WJ, Rasey JS, Evans ML, Grierson JR, Lewellen TK, Graham MM, et al. Imaging of hypoxia in human tumors with [F-18]fluoromisonidazole. Int J Radiat Oncol Biol Phys 1992;22:199–212.
[105] Casciari JJ, Graham MM, Rasey JS. A modeling approach for quantifying tumor hypoxia with [F-18]fluoromisonidazole PET time-activity data. Med Phys 1995;22:1127–39.
[106] Chapman JD, Schneider RF, Urbain JL, Hanks GE. Single-photon emission computed tomography and positron-emission tomography assays for tissue oxygenation. Semin Radiat Oncol 2001;11:47–57.
[107] Nunn A, Linder K, Strauss HW. Nitroimidazoles and imaging hypoxia. Eur J Nucl Med 1995;22:265–80.
[108] Biskupiak JE, Krohn KA. Second generation hypoxia imaging agents [editorial; comment]. J Nucl Med 1993;34:411–3.
[109] Kachur AV, Dolbier Jr WR, Evans SM, Shiue CY, Shiue GG, Skov KA, et al. Synthesis of new hypoxia markers EF1 and [18F]-EF1. Appl Radiat Isot 1999;51:643–50.
[110] Tewson TJ. Synthesis of [18F]fluoroetanidazole: a potential new tracer for imaging hypoxia. Nucl Med Biol 1997;24:755–60.
[111] Wiebe LI, Stypinski D. Pharmacokinetics of SPECT radiopharmaceuticals for imaging hypoxic tissues. Q J Nucl Med 1996;40:270–84.
[112] Siim BG, Laux WT, Rutland MD, Palmer BN, Wilson WR. Scintigraphic imaging of the hypoxia marker (99m)technetium-labeled 2,2′-(1,4-diaminobutane)-bis(2-methyl-3-butanone) dioxime (99mTc-labeled HL-91; prognox): noninvasive detection of tumor response to the antivascular agent 5,6-dimethylxanthenone-4-acetic acid. Cancer Res 2000;60:4582–8.
[113] Rumsey WL, Kuczynski B, Patel B, Bauer A, Narra RK, Eaton SM, et al. SPECT imaging of ischemic myocardium using a technetium-99m-nitroimidazole ligand. J Nucl Med 1995;36:1445–50.
[114] Zhang X, Melo T, Ballinger JR, Rauth AM. Studies of 99mTc-BnAO (HL-91): a non-nitroaromatic compound for hypoxic cell detection. Int J Radiat Oncol Biol Phys 1998;42:737–40.
[115] Stypinski D, Wiebe LI, McEwan AJ, Schmidt RP, Tam YK, Mercer JR. Clinical pharmacokinetics of 123I-IAZA in healthy volunteers. Nucl Med Commun 1999;20:559–67.
[116] Shelton ME, Green MA, Mathias CJ, Welch MJ, Bergmann SR. Assessment of regional myocardial and renal blood flow with copper-PTSM and positron emission tomography. Circulation 1990;82:990–7.
[117] Lewis JS, McCarthy DW, McCarthy TJ, Fujibayashi Y, Welch MJ. Evaluation of Cu-64-ATSM in vitro and in vivo in a hypoxic model. J Nucl Med 1999;40:177–83.
[118] Dehdashti F, Mintun MA, Lewis JS, Bradley J, Govindan R, Laforest R, et al. In vivo assessment of tumor hypoxia in lung cancer with 60Cu-ATSM. Eur J Nucl Med Mol Imaging 2003;30:844–50.
[119] Fujibayashi Y, Taniuchi H, Yonekura Y, Ohtani H, Konishi J, Yokoyama A. Copper-62-ATSM: a new hypoxia imaging agent with high membrane permeability and low redox potential. J Nucl Med 1997;38:1155–60.
[120] Ballinger JR. Imaging hypoxia in tumors. Semin Nucl Med 2001;31:321–9.
[121] Gabalski EC, Adam M, Pinto H, Brown JM, Bloch DA, Terris DJ. Pretreatment and midtreatment measurement of oxygen tension levels in head and neck cancers. Laryngoscope 1998;108:1856–60.
[122] Klabbers BM, Lammertsma AA, Slotman BJ. The value of positron emission tomography for monitoring response to radiotherapy in head and neck cancer. Mol Imaging Biol 2003;5:257–70.
[123] Alber M, Paulsen F, Eschmann SM, Machulla HJ. On biologically conformal boost dose optimization. Phys Med Biol 2003;48:N31–5.
[124] Ling CC, Humm J, Larson S, Amols H, Fuks Z, Leibel S, et al. Towards multidimensional radiotherapy (MD-CRT): biological imaging and biological conformality. Int J Radiat Oncol Biol Phys 2000;47:551–60.
[125] Tome WA, Fowler JF. Selective boosting of tumor subvolumes. Int J Radiat Oncol Biol Phys 2000;48:593–9.
[126] Peters LJ. Targeting hypoxia in head and neck cancer. Acta Oncol 2001;40:937–40.
[127] Solomon B, McArthur G, Cullinane C, Zalcberg J, Hicks R. Applications of positron emission tomography in the development of molecular targeted cancer therapeutics. BioDrugs 2003;17:339–54.
[128] Klimas MT. Positron emission tomography and drug discovery: contributions to the understanding of pharmacokinetics, mechanism of action and disease state characterization. Mol Imaging Biol 2002;4:311–37.
[129] Hammond LA, Denis L, Salman U, Jerabek P, Thomas Jr CR, Kuhn JG. Positron emission tomography (PET): expanding the horizons of oncology drug development. Invest New Drugs 2003;21:309–40.